Optical activity in planar chiral metamaterials: Theoretical study

Benfeng Bai,* Yuri Svirko, Jari Turunen, and Tuomas Vallius
University of Joensuu, Department of Physics and Mathematics, P.O. Box 111, FI-80101 Joensuu, Finland
(Received 14 March 2007; published 15 August 2007)

A thorough theoretical study of the optical activity in planar chiral metamaterial (PCM) structures, made of both dielectric and metallic media, is conducted by the analysis of gammadion-shaped nanoparticle arrays. The general polarization properties are first analyzed from an effective-medium perspective, by analogy with natural optical activity, and then verified by rigorous numerical simulation, some of which are corroborated by previous experimental results. The numerical analysis suggests that giant polarization rotation (tens of degrees) may be achieved in the PCM structures with a thickness of only hundreds of nanometers. The artificial optical activity arises from circular birefringence induced by the structural chirality and is enhanced by the guided-mode or surface-plasmon resonances taking place in the structures. There are two polarization conversion types in the dielectric PCMs, whereas only one type in the metallic ones. Many intriguing features of the polarization property of PCMs are also revealed and explained: the polarization effect is reciprocal and vanishes in the symmetrically layered structures; the effect occurs only in the transmitted field, but not in the reflected field; and the polarization spectra of two enantiomeric PCM structures are mirror symmetric to each other. These remarkable properties pave the way for the PCMs to be used as polarization elements in new-generation integrated optical systems.

DOI: 10.1103/PhysRevA.76.023811 PACS number(s): 42.25.Ja, 78.20.Ek, 78.67.Bf, 42.79.Dj

I. INTRODUCTION

The polarization direction of a linearly polarized plane wave can be rotated as it passes through some natural materials, such as quartz and solutions of chiral molecules; the effect is referred to as optical activity. In natural chiral media the optical activity arises from circular birefringence caused by the spatial dispersion of optical response either in chiral molecules or in chiral arrangements of molecules (molecular chirality). However, since the specific rotation (i.e., the rotation angle per unit thickness) of natural chiral materials is relatively low, one has to use thick bulk media to generate large polarization rotation. This is inconvenient in practical applications and, in particular, incompatible with the miniaturization requirement of new-generation optical systems.

In recent years, a new class of artificial materials, known as planar chiral metamaterials (PCMs, such as arrays of gammadion-shaped nanoparticles shown in Fig. 1), have invoked much interest in the scientific community due to their intriguing polarization properties: large optical activity and polarization conversion can be achieved in a PCM structure with a thickness of only a fraction of a wavelength [1–6]. In PCM structures the optical activity is not induced by molecular chirality but through structural chirality, i.e., by artificially chiral structural features in subwavelength scale. Since the strength of optical activity of PCMs is correlated to the degree of planar structural chirality [7], it is possible to optimize the polarization response of PCMs by proper structural design. Therefore, novel compact polarization elements based on PCMs appear feasible.

The investigation of PCMs started from metallic structures because the enhanced polarization effect was believed to be related to surface-plasmon resonances [1,3,4]. Papakostas *et al.* [1] observed diffraction and polarization conversion by metallic gammadion arrays and found rotation in excess of 30° in nonzero orders. Vallius *et al.* [2] showed later that polarization rotation in the zero-order transmitted wave at normal incidence is also possible, which resembles natural optical activity much more closely. Kuwata-Gonokami *et al.* [3,4] investigated the spectral dependence

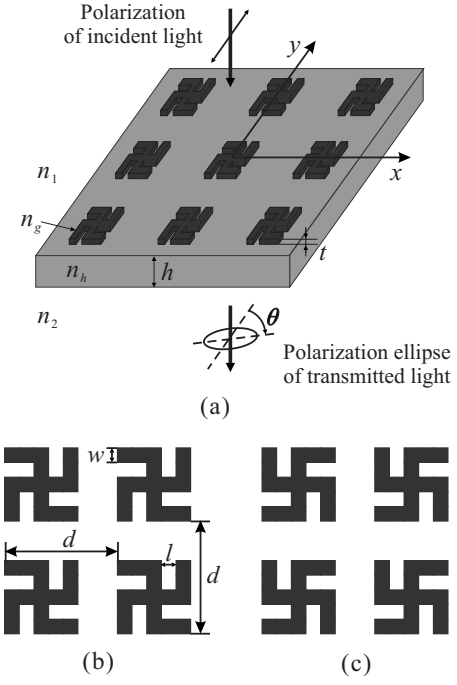

FIG. 1. Geometry of a PCM structure with an array of gammadion-shaped nanoparticle islands on a homogeneous layer. The polarization rotation of the zero-order transmitted wave is schematically shown in (a). (b) and (c) illustrate the top view of the left- and right-twisted gammadion structures. The notations of structural parameters are also indicated.

*bai@joyx.joensuu.fi

of polarization conversion effect in gold gammadion structures and observed large specific rotation ($\sim 10^4$°/mm) in direct transmission at normal incidence. The effect was further verified to be reciprocal, which also resembles natural optical activity.

Recently, Zhang *et al.* [5,6] reported their observation of polarization rotation in all-dielectric PCMs and suggested that multiple reflections within the chirally patterned layer, other than surface-plasmon resonances, may also play an important role in polarization conversion. This is undoubtedly a forward step to the full understanding of the underlying mechanism of the polarization effect in PCMs. However, Zhang *et al.* still did not detect any polarization change in the zero-order beam in either reflection or transmission, and explained this by arguments based on the effect of parity and time-reversal symmetry transformations.

In this paper, a thorough theoretical study of the polarization properties of both dielectric and metallic PCMs are performed by use of a rigorous numerical analysis method for crossed gratings. It is shown, at least theoretically, that PCMs are capable of producing large polarization rotation in the zero-order transmitted beam provided that appropriate resonance structures are designed. The phenomenological characteristics of the polarization spectra of PCMs are demonstrated and analyzed along with physical explanations. This paper aims to study in theory the general features of the polarization property of PCMs, which explain our previous experimental observations as well as line out our future investigation.

The paper is organized as follows. In Sec. II, we first analyze phenomenologically the origin of the optical activity in PCMs with an effective-medium approach, by analogy with natural optical activity, and thereby predict some basic features of the effect. Then, in Sec. III, the optical responses of gammadion-shaped nanostructures made of both dielectric and metallic materials are simulated numerically: the obtained polarization spectra verify the theoretical predictions. Section IV contains further discussion and explanation of the characteristics of the simulated spectra, providing a clearer understanding of the polarization behavior of PCMs. Finally, Sec. V summarizes the paper.

II. EFFECTIVE-MEDIUM ANALYSIS

To have a general insight into the optical activity in PCMs, we first examine it by analogy with the natural optical activity from an effective-medium perspective. The well-established electromagnetic theory of natural optical activity [8,9] indicates that the effect arises from the spatial dispersion in bulk chiral media, the chirality being induced either by molecules with inherent helical character or by helical arrangement of the atomic or molecular constituents. Therefore, in chiral media, the electric displacement vector $\mathbf{D}$ and the electric vector $\mathbf{E}$ should bear a relation [10]

$$\mathbf{D} = \epsilon \mathbf{E} + i\mathbf{G} \times \mathbf{E}, \tag{1}$$

where ϵ is the unperturbed permittivity tensor in achiral media and $\mathbf{G}=G\hat{\mathbf{k}}$ ($\hat{\mathbf{k}}$ is the unit wave vector) is the gyration vector responsible for the mechanism producing optical activity. Obviously, the gyration vector $\mathbf{G}$ is parallel to the wave vector $\mathbf{k}$, but its amplitude G is related to both the magnitude and direction of $\mathbf{k}$ (because of spatial dispersion). The cross product $\mathbf{G}\times\mathbf{E}$ can be represented as the product of an antisymmetric tensor $[G]$ with $\mathbf{E}$, i.e.,

$$\mathbf{G} \times \mathbf{E} = \begin{pmatrix} 0 & -G_z & G_y \\ G_z & 0 & -G_x \\ -G_y & G_x & 0 \end{pmatrix} \mathbf{E} \equiv [G]\mathbf{E}, \tag{2}$$

where G_x, G_y, and G_z are rectangular components of $\mathbf{G}$. Then from Eqs. (1) and (2) we can derive

$$\mathbf{D} = (\epsilon + i[G])\mathbf{E} \equiv \epsilon' \mathbf{E}, \tag{3}$$

where ϵ' is the permittivity tensor of the chiral medium.

Since G is a function of the propagation direction of light, it can be expanded as a quadratic equation of the direction cosines of the unit wave vector $\hat{\mathbf{k}}=(s_x,s_y,s_z)$:

$$G = g_{11}s_x^2 + g_{22}s_y^2 + g_{33}s_z^2 + 2g_{12}s_x s_y + 2g_{23}s_y s_z + 2g_{31}s_z s_x, \tag{4}$$

where the coefficients g_{ij} form a symmetric tensor $[g_{ij}]$ known as the gyration tensor [10]. The gyration tensor describes the optical activity of chiral materials; its zero elements can be determined from the symmetry properties of materials. For example, for a uniaxial crystal with fourfold rotational symmetry (but no centrosymmetry) about the optical axis in the z direction, the elements of the gyration tensor are $g_{11}=g_{22}$, $g_{12}=g_{23}=g_{31}=0$ [10]. Suppose that the light also propagates along z direction, i.e., $\hat{\mathbf{k}}=\hat{\mathbf{z}}$. Then, from Eq. (4) and the definition of $\mathbf{G}$, we can derive $G_z=g_{33}$ and $G_x=G_y=0$. Therefore Eqs. (2) and (3) lead to

$$\mathbf{D} = \epsilon' \mathbf{E} = \begin{pmatrix} n_o^2 & -ig_{33} & 0 \\ ig_{33} & n_o^2 & 0 \\ 0 & 0 & n_e^2 \end{pmatrix} \mathbf{E}, \tag{5}$$

where n_o and n_e are the principal refractive indices of the uniaxial crystal.

If the waves propagating in the material are right- (RCP) and left-circularly polarized (LCP), with electric vectors denoted by $\mathbf{E}_\pm = E_0(\hat{\mathbf{x}} \pm i\hat{\mathbf{y}})$, Eq. (5) gives

$$\mathbf{D}_\pm = (n_o^2 \pm g_{33})\mathbf{E}_\pm \equiv n_\pm^2 \mathbf{E}_\pm. \tag{6}$$

Equation (6) shows that the propagation of the RCP and LCP waves in chiral media is just like that in isotropic media except that the two waves experience different refractive indices, which causes a difference in their phase velocities; this is called circular birefringence. Therefore, the recombination of the RCP and LCP components of a linearly polarized wave after a passage through a chiral medium gives an elliptically polarized wave, and the major axis of the polarization ellipse is in general rotated. This is the origin of natural optical activity.

The PCMs are very similar to natural chiral media in the sense that they are also composed of chiral microstructures (such as the gammadion particles in Fig. 1) that can be regarded as macroscopic chiral "molecules" because their di-

mensions are much larger than those of real molecules. However, when the structural dimensions are small enough, especially when comparable with or smaller than the illumination wavelength, the PCMs are no more than manmade chiral two-dimensional crystals. Therefore, from an effective-medium viewpoint, the optical activity in PCMs should originate from the optical spatial dispersion caused by structural chirality, which resembles natural optical activity arising from molecular chirality. On this basis, some fundamental features of the optical activity in PCMs may be prefigured.

We analyze in this paper the PCM structure shown in Fig. 1, where an array of gammadion-shaped nanoparticle islands with period $d \times d$ and thickness t is located on a homogeneous layer of thickness h. The refractive indices of the upper space, the substrate, the homogeneous layer, and the gammadions are denoted by n_1, n_2, n_h, and n_g, respectively. The gammadion pattern can be either left [Fig. 1(b)] or right twisted [Fig. 1(c)], which is of plane group $p4$ and has the C_4 (fourfold rotational) symmetry about the z axis [11]. Therefore, with effective-medium theory, the gammadion layer can be regarded as a uniaxial crystal with its optical axis along the z direction. If we define an effective permittivity tensor $\boldsymbol{\epsilon}'_{\text{eff}}$ for the gammadion layer, it should certainly have the form of Eq. (5), provided that the light also propagates in the z direction. In that case, circular birefringence would also occur in the gammadion layer, as described by Eq. (6).

It is necessary to note that, according to the symmetries of the structure and the normal incidence condition, it is easy to prove that the circularly polarized waves are eigenmodes of the structure, i.e., illuminating the structure with a RCP or LCP wave produces still circularly polarized reflected or transmitted waves. So the description of circular birefringence in the PCMs with Eq. (6), in an effective-medium approach, is appropriate.

Now let us concentrate on the polarization property of the zero-order transmitted beam when a linearly polarized plane wave is normally incident on the structure. We define the complex transmission coefficients of the RCP (+) and LCP (−) components as

$$t_{\pm} = a_{\pm} \exp(i\phi_{\pm}), \tag{7}$$

where the real quantities $a_{\pm}$ and $\phi_{\pm}$ are the amplitudes and phases of $t_{\pm}$, respectively. Then the polarization rotation angle θ (i.e., the angle between the long axis of the transmitted polarization ellipse and the incident polarization direction) can be simply expressed as

$$\theta = \frac{1}{2}(\phi_+ - \phi_-) \tag{8}$$

and the ellipticity angle χ is given by

$$\tan \chi = \frac{a_+ - a_-}{a_+ + a_-}. \tag{9}$$

These equations imply that the polarization rotation and the induced ellipticity are caused by the splitting of phase spectra and the splitting of amplitude spectra, respectively. A similar analysis can also be carried out for the reflected field.

Following the physical description of the structural optical activity, we can also predict logically three main features of the polarization property of PCMs.

A. Reciprocity of the polarization effect

As mentioned above, the gyration vector **G** is parallel to the wave vector **k**, meaning that the reversion of the propagating direction of light changes the sign of tensor $[G]$ in Eq. (2). According to Eqs. (5) and (6), this would lead to an interchange of the values of n_+ and n_-, which consequently reverses the polarization rotation direction in the global coordinate system. This implies that the sense of rotation bears a fixed relation to the propagation direction of light for a given PCM structure. In other words, if a linearly polarized beam is reflected back on itself, the net rotation would be zero. So the optical activity in PCMs is a reciprocal effect.

B. Polarization rotation vs handedness

In the PCMs that we are considering, the effective parameter G_{eff} should be a function of both **k** and the chirality index ξ of the structure. Here ξ is a measure of the degree of structural chirality, which can be calculated by using, for example, the model proposed by Potts *et al.* [7] In particular, when the handedness of the gammadion pattern is reversed, ξ changes sign and the sign of G_{eff} is changed as well, which results in the reversion of the polarization rotation direction [see Eq. (6)]. Actually, this point is easy to arrive at with a symmetry logic: at normal incidence, two enantiomeric PCMs as well as the incident fields are the mirror images of each other; consequently their polarization rotation responses should also be mirror symmetric, i.e., in opposite directions. Therefore, the polarization spectra of two enantiomeric PCMs should be mirror symmetric to each other about the 0° axis.

C. Polarization effect in symmetrically layered PCMs

As long as features 1 and 2 are recognized, feature 3 is just a deduction from them. In a PCM structure with symmetric configuration in the z direction, i.e., the structure being mirror symmetric about the xy plane, neither polarization rotation nor elliptization can happen. The logic is quite simple: for the z-symmetric PCMs, the incidences on two enantiomeric structures are just the same as those on one of them, but from the front and back sides. According to feature 1, the polarization rotation direction remains the same with respect to the direction of light no matter whether it is incident on the front or back side of the structure; whereas according to feature 2, the rotation directions should be opposite for two enantiomeric PCMs. So the final result is that the polarization rotation angle is zero. Furthermore, according to the reciprocity theorem of electromagnetism [12], the transmission coefficient of a RCP wave (t_+) remains the same no matter whether it impinges on the front or back side of a PCM structure. However, the latter situation is just the mirror counterpart of a LCP wave impinging on the front side of the same PCM, both of which should have the same transmis-

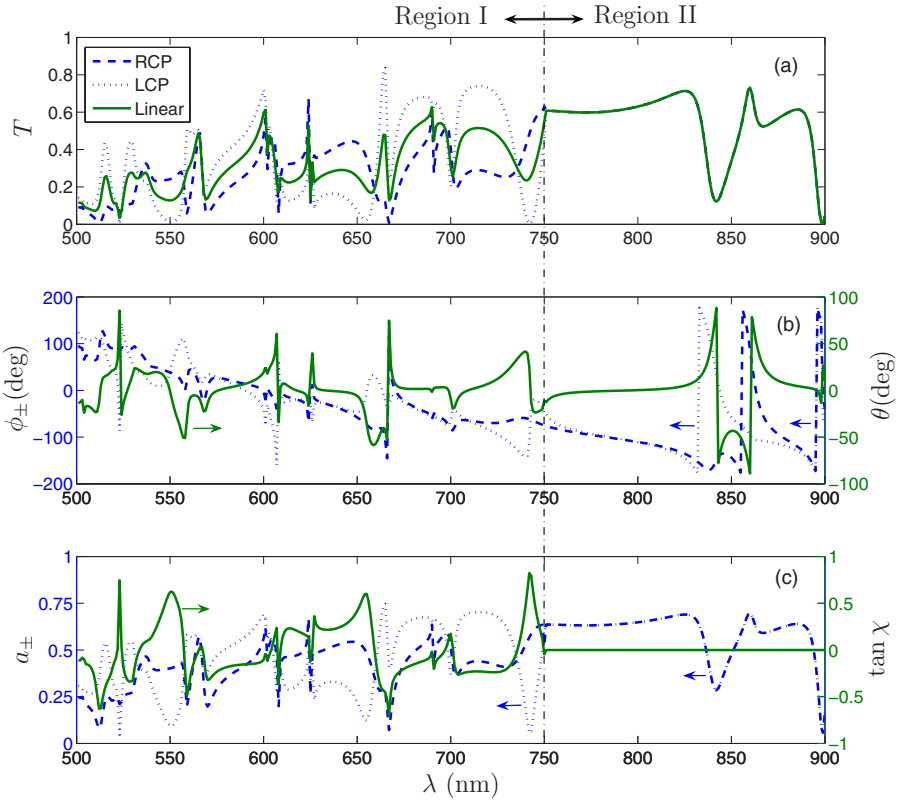

FIG. 2. (Color online) Spectra of a dielectric gammadion PCM structure: (a) the transmittance of a linearly polarized wave and its RCP and LCP components; (b) the phases $\phi_\pm$ of the transmission coefficients $t_\pm$ and the polarization rotation angle θ; (c) the amplitudes $a_\pm$ of $t_\pm$ and the ellipticity tan χ. Dashed, dotted, and solid lines refer to RCP, LCP, and linearly polarized illuminations, respectively. The arrows in (b) and (c) indicate whether the left or right scales should be considered.

sion coefficients. So we get $t_+=t_-$ in this case, which leads to $\chi=0$ according to Eq. (9).

Although we have predicted some general properties of PCMs, the effective-medium approach is after all an approximation, and therefore the real polarization properties of PCMs should be investigated either by rigorous numerical simulation or experimentally. In the next section we perform the numerical analysis of the polarization response of gammadion PCMs, some aspects of which are verified by recent experimental results.

III. NUMERICAL SIMULATION

The method used to calculate the optical response of gammadion PCMs is the reformulated Fourier modal method for crossed gratings with C_4 symmetry [13]. It is well known that the Fourier modal method (also known as the rigorous coupled-wave approach) is one of the most efficient and versatile rigorous numerical methods for gratings. The method adopted here benefits from a group-theoretic approach [14] with C_4 symmetry consideration, whose computation time and memory occupation are reduced to 1/32 and 1/4 at normal incidence, in comparison with the traditional Fourier modal method [15]. Since the PCM structures considered are no more than crossed gratings with C_4 symmetry, the present method is the most appropriate to perform fast and well-converged simulation, especially for the metallic PCMs. In the following, the gammadion PCMs made of both dielectric and metallic materials are analyzed in detail.

A. Dielectric gammadion structures

We first investigate all-dielectric gammadion PCMs as shown in Fig. 1. To demonstrate the general features of the polarization property, we analyze here a representative structure with left-twisted gammadions [see Fig. 1(b)], where $d=500$ nm, $w=l=80$ nm, $h=t=200$ nm, $n_1=1$, $n_2=1.5$, and $n_g=n_h=3$. The refractive indices of materials are chosen such that guided-mode resonances can take place in the structure. In the calculation, the normally incident light is assumed to be y polarized, although the polarization rotation effect is independent of the incident polarization angle due to circular birefringence, which is also verified by numerical simulation. So the rotation angle θ is evaluated within $[-90°, 90°]$.

Figure 2 shows the simulated zero-diffraction-order spectra of the transmittance T, polarization rotation angle θ, and ellipticity tan χ of the structure. It is seen that giant polarization rotation (as large as tens of degrees) can be produced near the resonance wavelengths. The spectra in Figs. 2(b) and 2(c) satisfy the relations given by Eqs. (8) and (9) well, which confirms that the polarization rotation and elliptization of the zero-order transmitted beam are indeed caused by circular birefringence taking place in the PCM structure, as is predicted in Sec. II. The transmittance of the total field [see Fig. 2(a)] also satisfies the relation $T=\frac{1}{2}(T_++T_-)$, where $T_\pm=(n_2/n_1)a_\pm^2$ are the transmittances of the RCP and LCP waves, which is valid for a uniform material. Furthermore, from the spectra, we can find many interesting polarization properties of the dielectric PCMs.

The most striking feature is that the spectra are clearly divided into two regions (denoted by I and II in Fig. 2) with respect to wavelength λ, according to their different polarization conversion properties. In region I, both the polarization rotation and elliptization take place, and the spectra obey the Kramers-Kronig (KK) relations [16] well (detailed discussion will be given in Sec. IV D); whereas, in region II,

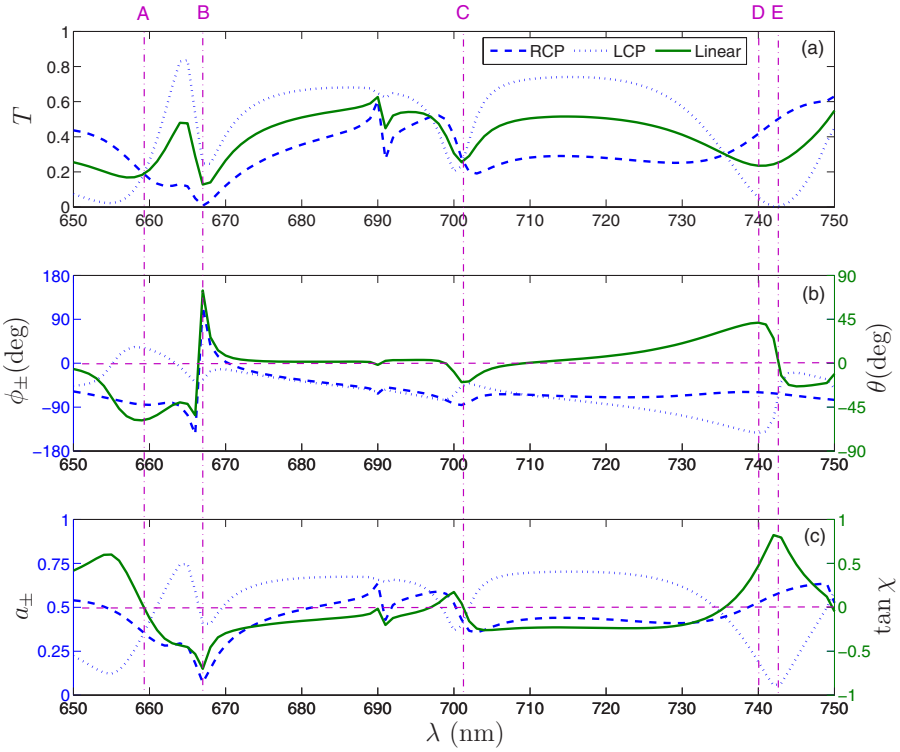

FIG. 3. (Color online) Type-I polarization rotation. The figure reads in the same way as Fig. 2. A, B, C, etc., indicate five characteristic wavelengths. The baselines of $\theta=0$ and $\tan\chi=0$ are displayed in (b) and (c).

the ellipticity angle χ is zero everywhere no matter the polarization rotation is excited or not, and the spectra do not satisfy the KK relations any more. The division point between the two spectral regions is $\lambda_0=n_2d=750$ nm, beyond which no diffraction would occur (i.e., only the zeroth diffraction order exists) in the transmission side. The abrupt change of spectra at λ_0 is well known as the Rayleigh anomaly [17], which is caused by the redistribution of light energy when higher diffraction orders vanish at this wavelength.

Although the two polarization types are different, it is evident that they are both caused by the splitting of the RCP and LCP spectra: in region I, the splitting of $\phi_{\pm}$ and $a_{\pm}$ both occur, which cause both the polarization rotation and ellipticization; however, in region II, only $\phi_{\pm}$ split around the resonances and $a_{\pm}$ are always the same, which results in the vanishing of ellipticity.

Now let us take a closer look at the two polarization types. Figures 3 and 4 are the blowups of the type-I and type-II polarization spectra extracted from Fig. 2 in the regions $650\ \text{nm}<\lambda<750\ \text{nm}$ and $820\ \text{nm}<\lambda<880$ nm, respectively. It is seen that the locations of large polarization conversion are all associated with transmission peaks or dips (indicated by A-H in Figs. 3 and 4), implying that the polarization effect is substantially enhanced by the guided-mode resonances taking place in the structure. The guided-mode resonance is a common property of planar dielectric waveguide gratings: at resonance, energy from an incident wave is coupled into a leaky mode and then back into one or more radiation modes, producing sharp transmission (or reflection) peaks or dips [18,19]. Since the PCMs considered are no more than crossed waveguide gratings, the guided-mode resonance can, of course, be excited, exhibiting a transmission peak or dip depending on whether constructive or destructive interference takes place in the transmitted field. However, it is still not clear for us how the resonance physically affects the polarization rotation, which will be investigated in our future work. It is also necessary to emphasize that the polarization rotation can still happen even without the waveguide because the effect is caused by structural chirality, but the rotation angle is much smaller.

Table I gives the specific values of T, θ and $\tan\chi$ at the eight characteristics wavelengths λ. We can see that, in region I, some types of polarization conversion can be achieved due to the elliptization. For example, at λ_A and λ_C, pure linear polarization rotation as large as $-58.38°$ and $-20.28°$ can be realized because $\chi=0$ at these wavelengths. At λ_B and λ_E, the PCM structure behaves similar to a quarter wave plate, which can produce a nearly circularly polarized wave (note that $\tan\chi$ is also the ratio of the short axis to the long axis of the polarization ellipse). Finally, at λ_D, the polarization direction is rotated by about 45° with the ellipticity $\tan\chi=0.47$, which is quite similar to the effect of an 1/8-wave plate.

In region II, only pure linear polarization rotation can be realized because the ellipticity is always zero. However, the rotation occurs no longer only at some isolated wavelengths as in region I, but over a substantial wavelength range around the resonance. For example, in Fig. 4 we can get the maximum rotation angle of 136.75° at λ_G, which corresponds to a giant specific rotation of $3.4\times10^5\,°/\text{mm}$. Therefore any angle between 0 and this maximum can be achieved at other wavelengths. Specially, at λ_F and λ_H, the gammadion structure produces pure 90° polarization rotation, as a half wave plate does.

The above analysis shows that multiple functions of polarization control may be realized with dielectric PCMs, in which the polarization conversion is effectively enhanced by

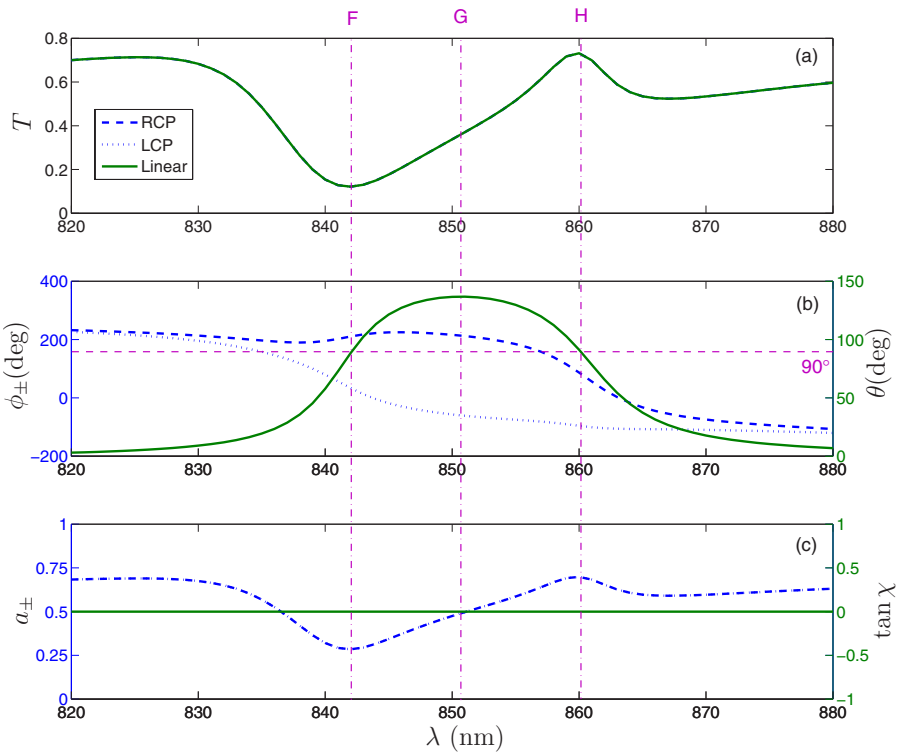

FIG. 4. (Color online) Type-II polarization rotation. The figure reads in the same way as Fig. 2. F, G, and H indicate three characteristic wavelengths. The baseline of θ=90° is displayed in (b). Please note that, for convenience of reading, the evaluation range of θ has been converted from [−90°, 90°] to [0°, 180°] and the ranges of $\phi_{\pm}$ are adjusted as well in this figure.

guided-mode resonances. However, it is necessary to note that although guided-mode resonances also happen in the reflected field, there is no polarization conversion at all, which has been verified by our numerical simulation. The reason for this interesting phenomenon as well as the origin of generating the two polarization types in transmission will be discussed in detail in Sec. IV. We proceed to check numerically whether the three features predicted in Sec. II are correct.

We first recalculate the transmission spectra of the left-twisted gammadion array analyzed above, but with the incident light from the opposite side of the structure. The obtained results (including the transmittance T, the polarization rotation angle θ and the ellipticity tan χ) are exactly the same as those shown in Fig. 2, meaning that the optical response does not depend on whether the light is incident from the upper or lower side of the same PCM structure. So the polarization conversion in dielectric PCMs is indeed a reciprocal effect.

TABLE I. Values of T, θ, and tan χ at the eight characteristics wavelengths λ indicated in Figs. 3 and 4.

Point	λ (nm)	T	θ (deg)	tan χ
A	659.2	0.19	−58.38	0.00
B	666.9	0.13	83.06	−0.70
C	701.2	0.26	−20.28	0.00
D	740.0	0.24	41.59	0.47
E	742.6	0.25	−0.26	0.84
F	842.1	0.12	89.81	0.00
G	850.7	0.36	136.75	0.00
H	860.1	0.73	89.96	0.00

Then let us consider two enantiomeric PCM structures: the one analyzed above and a similar one but with right-twisted gammadions [see Fig. 1(c)]. A normal-incidence condition from the upper space is assumed for both of them. The calculated spectra in the wavelength range 680 nm$<\lambda<$780 nm are shown in Fig. 5. It is evident that, as the transmittance remains the same for the two enantiomeric PCMs, both the polarization rotation and ellipticity spectra of them are mirror symmetric to each other about the 0° axis, in line with the predicted feature 2. Therefore, the handedness of the chiral structure substantially affects the direction of polarization rotation.

Finally, to analyze a structure with symmetric configuration in z direction, we assume h=0 and n_1=n_2=1.5 in the above considered left-twisted PCM. The structure is therefore simply an array of gammadions buried in a homogeneous dielectric medium. Figure 6 shows its transmission and polarization spectra, from which we can see that neither polarization rotation nor elliptization occur in this case. The simulation results also coincide with the theoretical prediction well.

We emphasize that the polarization response of PCMs is largely affected by factors such as structural dimensions, pattern perfectness, material properties, and illumination conditions. Therefore, a proper structural design is quite essential to generate required polarization properties. For example, Zhang *et al.* [5,6] reported that they failed to detect any discernable change of polarization in the zero-order beam when the dielectric gammadion samples with a period of 5 μm (several times larger than the illumination wavelength) were illuminated with 632 nm linearly polarized wave at normal incidence. We have also simulated their structures numerically with the given parameters, and found that the polarization rotation angle of the zero-order transmitted

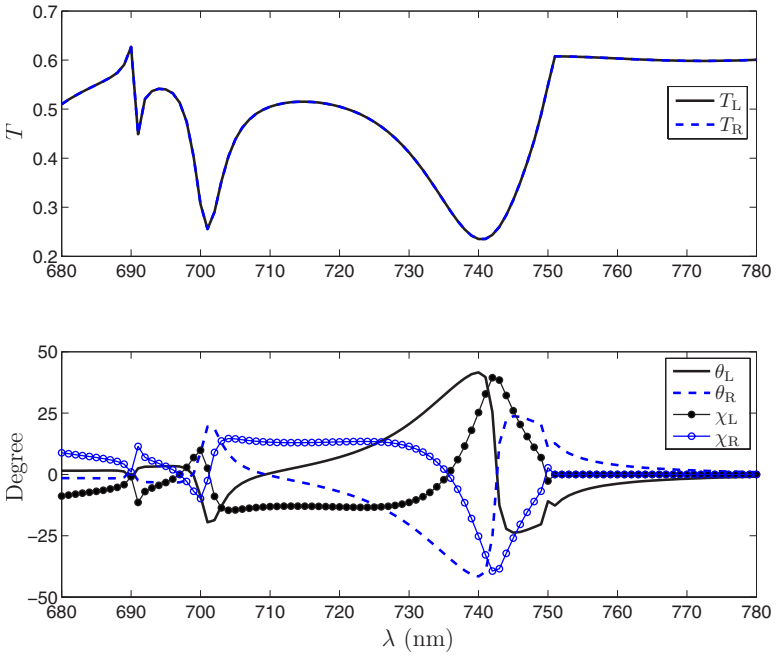

FIG. 5. (Color online) Transmission and polarization spectra of two enantiomeric PCM structures. The subscripts *L* and *R* refer to the left- and right-twisted gammadion arrays, respectively.

beam is really as small as 10^{-2}°, which is indeed hard to detect. So, the absence of polarization rotation in their zero-order transmission is not an intrinsic property of the PCMs, but just due to the improper design of the structures. Although an in-depth investigation of the correlation between the polarization effect and the structural parameters is quite necessary, especially for the optimization of the polarization property of the PCMs, it is more similar to an engineering task and will be addressed elsewhere.

B. Metallic gammadion structures

We proceed to simulate metallic PCMs, where the gammadion particles and the homogeneous layer are both gold, i.e., $n_g = n_h = n_{\mathrm{Au}}$. The refractive-index values of gold are obtained by interpolation between the tabulated data given in Ref. [20]. The other structural parameters are chosen as $d = 500$ nm, $w = l = 80$ nm, and $n_1 = n_2 = 1.5$, while t and h are changeable.

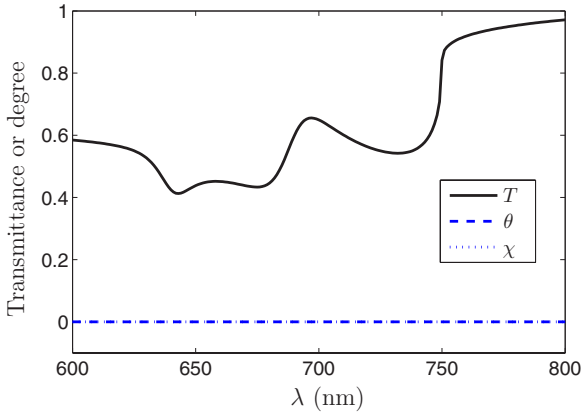

FIG. 6. (Color online) Transmission and polarization spectra of the left-twisted PCM with symmetric configuration in the *z* direction.

Figure 7 demonstrates the transmittance and polarization spectra of the left-twisted gold gammadion structures, where $t = 150$ nm and h is varied between 0 and 30 nm. Figure 8 gives the corresponding spectra if $h = 15$ nm and t is varied between 50 and 200 nm. The results show that large polarization rotation (up to 25°, implying specific rotation of 1.5×10^5°/mm) can be achieved in the metallic gammadion structures, provided that a proper set of structural parameters are adopted. It is also evident that the polarization peaks always occur in the vicinity of the surface-plasmon resonances, no matter what values of h and t are chosen. In other words, the polarization rotation in the metallic PCMs is substantially enhanced by the surface-plasmon resonances. Therefore, to get large polarization rotation, the structure design should be optimized so as to effectively excite a surface-plasmon resonance.

However, it is seen that, at the wavelengths where large polarization rotation occurs, the transmittance is often quite low (compared to the spectra of the dielectric PCMs). This is a major disadvantage for the application of the metallic PCMs. Therefore it seems that the dielectric PCMs are more suitable to be developed as practical polarization elements because of their better performance as well as easier manufacturability.

The numerical simulation also reveals that the polarization spectra of the metallic PCMs possess most of the features of those of the dielectric PCMs: (i) the polarization spectra satisfy the relations of Eqs. (8) and (9) well, indicating the occurrence of circular birefringence; (ii) the polarization conversion effect takes place only in the transmitted field, but not in the reflected field; (iii) the polarization effect is reciprocal and vanishes in the structures with symmetric configuration in z direction (see the case of $h = 0$ shown in Fig. 7); and (iv) the polarization spectra of two enantiometric metallic PCM structures are mirror symmetric to each other.

By comparing with our previous experimental measurements on gold gammadion nanoparticle arrays [3], we can

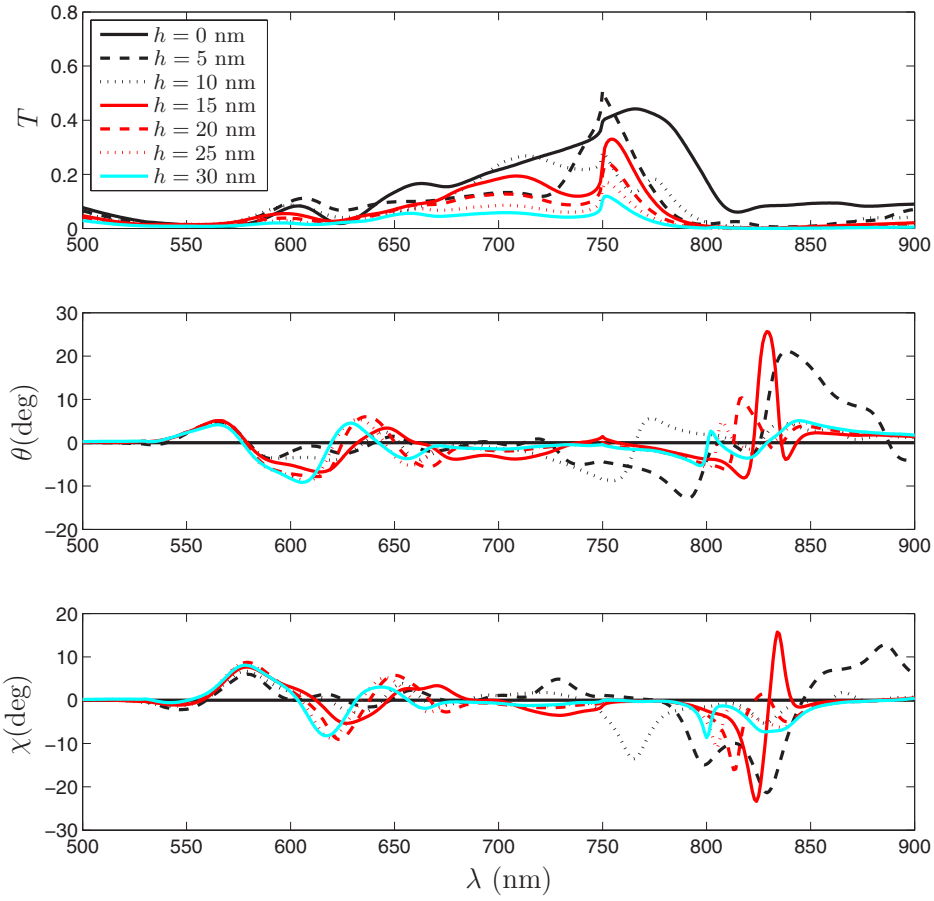

FIG. 7. (Color online) Transmittance and polarization spectra of left-twisted gold PCMs with $t = 150$ nm if h is varied between 0 and 30 nm.

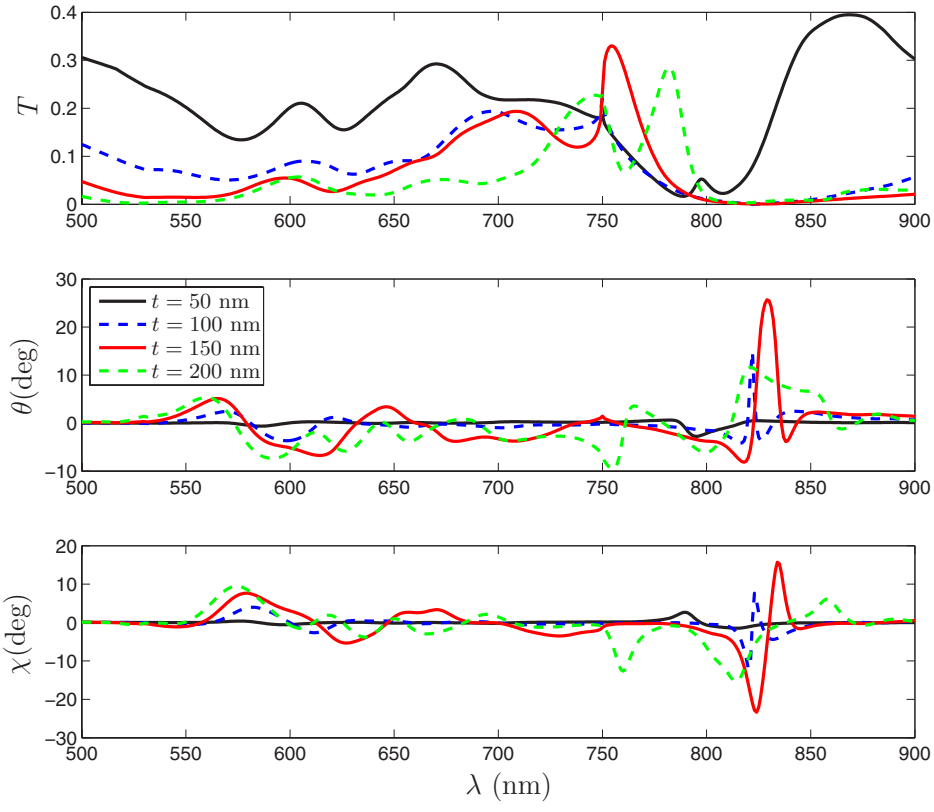

FIG. 8. (Color online) Transmittance and polarization spectra of left-twisted gold PCMs with $h = 15$ nm if t is varied between 50 and 200 nm.

see that the theoretically predicted features are in good agreement with our experimental observations (see Fig. 2 of Ref. [3]), in the aspects of large zero-order polarization rotation, the characteristic of surface-plasmon resonance enhancement, and the above mentioned features (iii) and (iv). We should confess that we failed to reproduce accurately the measured spectra by numerical simulation, because the gold gammadion structure is so complicated that its optical response is sensitive to many practical factors such as refractive index of gold particles, structural dimensions, and the perfectness of the gammadion pattern; hence the accurate simulation is almost impossible unless we can accurately know the specific values of all of these parameters. However, it does not prevent us from seeing the coincidence of the general features between theory and experiment.

It is necessary to note that although most of the polarization properties of metallic PCMs are similar to those of dielectric ones, there is one remarkable difference: the metallic PCMs have only one polarization type (i.e., the type-I rotation as shown in Figs. 7 and 8), therefore the spectra never divide into two regions as the spectra of the dielectric PCMs do. Accordingly, the spectra of θ and χ always satisfy the KK relations. A detailed discussion of this point will be presented in Sec. IV D.

IV. INTERPRETATION AND DISCUSSION

Having simulated the polarization spectra of both dielectric and metallic PCMs and realized their many intriguing features, we still have several unclear points to discuss, i.e., (i) the absence of polarization rotation in the reflected field, (ii) the zero ellipticity in the type-II region, and (iii) the reasons why the type-I spectra satisfy the KK relations, whereas the type-II spectra do not. In this section, we provide insight into these phenomena and, thereby, give reasonable interpretations.

A. Absence of polarization conversion in reflection

As shown above, there is no polarization rotation in the reflected field in either the dielectric or metallic PCMs. The phenomenon can be explained with the reciprocity theorem of electromagnetism [12].

First of all, we need to redefine two sets of (complex) reflection and transmission coefficients: one set consists of σ_{ss}, σ_{sp}, σ_{ps}, and $\sigma_{pp}(\sigma=r,t)$, which describe the polarization conversion between the s and p components of the incident and the zero-order diffracted waves; the other set includes σ_{++}, σ_{+-}, σ_{-+}, and $\sigma_{--}(\sigma=r,t)$, where r_{+-}, for example, gives the ratio of the reflected LCP amplitude to the incident RCP amplitude. With these coefficients, we can easily write out the diffracted field amplitudes for different incident waves, as shown in Table II. Note that the associated polarization basis vectors $\hat{\mathbf{s}}$ and $\hat{\mathbf{p}}$ are defined by

$$\hat{\mathbf{s}} = \frac{\mathbf{k}\times\hat{\mathbf{z}}}{|\mathbf{k}\times\hat{\mathbf{z}}|}, \quad \hat{\mathbf{p}} = \frac{\hat{\mathbf{s}}\times\mathbf{k}}{|\mathbf{k}|}. \tag{10}$$

From the last two equations in Table II, we can derive the relations between the two sets of coefficients:

TABLE II. Diffracted field amplitudes at different incidences.

Input	Output[a]
$\hat{\mathbf{s}}$	$\sigma_{ss}\hat{\mathbf{s}}'+\sigma_{sp}\hat{\mathbf{p}}'$
$\hat{\mathbf{p}}$	$\sigma_{ps}\hat{\mathbf{s}}'+\sigma_{pp}\hat{\mathbf{p}}'$
$\mathbf{E}_+=\hat{\mathbf{p}}+i\hat{\mathbf{s}}$	$(\sigma_{ps}\hat{\mathbf{s}}'+\sigma_{pp}\hat{\mathbf{p}}')+i(\sigma_{ss}\hat{\mathbf{s}}'+\sigma_{sp}\hat{\mathbf{p}}')$
	$=\sigma_{++}(\hat{\mathbf{p}}'+i\hat{\mathbf{s}}')+\sigma_{+-}(\hat{\mathbf{p}}'-i\hat{\mathbf{s}}')$
$\mathbf{E}_-=\hat{\mathbf{p}}-i\hat{\mathbf{s}}$	$(\sigma_{ps}\hat{\mathbf{s}}'+\sigma_{pp}\hat{\mathbf{p}}')-i(\sigma_{ss}\hat{\mathbf{s}}'+\sigma_{sp}\hat{\mathbf{p}}')$
	$=\sigma_{-+}(\hat{\mathbf{p}}'+i\hat{\mathbf{s}}')+\sigma_{--}(\hat{\mathbf{p}}'-i\hat{\mathbf{s}}')$

[a] $\hat{\mathbf{s}}'$ and $\hat{\mathbf{p}}'$ are the polarization basis vectors for the diffracted wave.

$$\sigma_{++} = \frac{1}{2}[(\sigma_{pp}+\sigma_{ss})+i(\sigma_{sp}-\sigma_{ps})],$$

$$\sigma_{+-} = \frac{1}{2}[(\sigma_{pp}-\sigma_{ss})+i(\sigma_{sp}+\sigma_{ps})],$$

$$\sigma_{-+} = \frac{1}{2}[(\sigma_{pp}-\sigma_{ss})-i(\sigma_{sp}+\sigma_{ps})],$$

$$\sigma_{--} = \frac{1}{2}[(\sigma_{pp}+\sigma_{ss})-i(\sigma_{sp}-\sigma_{ps})]. \tag{11}$$

Now let us consider two cases: (a) an incident wave with wave vector $\mathbf{k}_i^a$ and electric field amplitude $\mathbf{E}_i^a$ excites a zero-order diffracted field with wave vector $\mathbf{k}_d^a$ and electric field amplitude $\mathbf{E}_d^a$; (b) an incident wave with wave vector $\mathbf{k}_i^b=-\mathbf{k}_d^a$ and electric field amplitude $\mathbf{E}_i^b$ excites a zero-order diffracted field with wave vector $\mathbf{k}_d^b=-\mathbf{k}_i^a$ and electric field amplitude $\mathbf{E}_d^b$. Obviously, (a) and (b) are a pair of conjugate cases. Then the reciprocity theorem [12] tells us that

$$|\hat{\mathbf{z}}\cdot\mathbf{k}_i^a|(\mathbf{E}_i^a\cdot\mathbf{E}_d^b) = |\hat{\mathbf{z}}\cdot\mathbf{k}_d^a|(\mathbf{E}_i^b\cdot\mathbf{E}_d^a), \tag{12}$$

which is valid when the media in the upper space and the substrate are lossless. Equation (12) is very useful: by setting the electric field vectors of the two incident waves to be s or p polarized, one can easily obtain the relation between the polarization-conversion coefficients of any pair of conjugate incidence configurations. This work has been done by Li for bianisotropic gratings [21]. Since the gammadion structure has the C_4 symmetry, with the similar analysis process as that for theorem 1 in Ref. [21], we can get

$$r_{sp} = -r_{ps} \tag{13}$$

for any incident angle. Especially, for the reflection of a normally incident wave, $\hat{\mathbf{s}}'=\hat{\mathbf{s}}$ and $\hat{\mathbf{p}}'=-\hat{\mathbf{p}}$. Then, owing to the symmetry of the structure, we have

$$r_{sp} = r_{ps} = 0, \quad r_{ss} = -r_{pp}. \tag{14}$$

Substituting Eq. (14) into Eq. (11), we can derive

$$r_{++} = r_{--} = 0, \quad r_{+-} = r_{-+}. \tag{15}$$

Equation (15) shows that the complex reflection coefficients of the LCP and RCP waves are always the same no matter whether the gammadion structure is metallic or dielectric, provided that the incidence is normal and the structure has the perfect C_4 symmetry. This explains [with Eqs. (8) and (9)] why no polarization conversion takes place in the reflected field of the gammadion structures. However, if the C_4 symmetry of the structure is broken (say, due to the imperfectness of the fabricated sample) or the incidence is oblique, polarization rotation can occur in the reflected field, which has also been verified by our numerical simulation.

B. Absence of polarization conversion in the symmetrically layered structures

Following the same line of analysis as in Sec. IV A, we can also explain, from another point of view, why there is no polarization rotation in the transmitted field of the PCMs with symmetrical configuration in the z direction. In this case, the structure has the spatial inversion symmetry, i.e., the structure remains unchanged after the spatial reversal of all points with respect to a properly chosen coordinate origin. Then with the similar analysis process as that for theorem 2 in Ref. [21], we have

$$t_{sp} = t_{ps} \tag{16}$$

for any incident angle. For the special case of normal incidence, according to $\hat{\mathbf{s}}' = \hat{\mathbf{s}}$, $\hat{\mathbf{p}}' = \hat{\mathbf{p}}$, and the symmetry considerations, it can be shown that

$$t_{sp} = -t_{ps} = 0, \quad t_{ss} = t_{pp}. \tag{17}$$

Substituting Eq. (17) into Eq. (11), we have

$$t_{++} = t_{--}, \quad t_{+-} = t_{-+} = 0, \tag{18}$$

meaning that the complex transmission coefficients of the LCP and RCP waves are the same. Therefore, according to Eqs. (8) and (9), there is no polarization conversion in the transmitted field, which coincides with our theoretical prediction and numerical simulation. However, similarly, if the C_4 symmetry of the structure is broken or the incidence is not normal, the polarization rotation would be recovered.

C. Zero ellipticity in the type-II polarization

With the conclusion in Sec. IV A, we can easily understand the behavior of the type-II polarization rotation. For a dielectric structure with the illumination wavelength larger than the diffraction limit λ_0 (see Sec. III A), there are only the zero-order reflected and transmitted diffraction waves. Since the reflectances of the LCP and RCP waves are the same due to Eq. (15) and $R=|r|^2$, their transmittances are also the same due to energy conservation in lossless media (i.e., $T=1-R$). So, according to $T=|t|^2$, the amplitudes of the complex transmission coefficients of the LCP and RCP waves are the same, which leads to zero ellipticity due to Eq. (9). Therefore, once the illumination wavelength falls into the type-II region, the ellipticity is always zero.

However, the deduction is not applicable to the metallic PCMs because the media are absorptive. This may also explain why there is no type-II polarization rotation in the metallic PCMs.

D. Comments on the Kramers-Kronig relations

The KK relations are a consequence of strict causality, i.e., the effect cannot precede the cause. In the theory of optical activity, the optical rotatory dispersion spectra (namely, the θ spectra) and the circular dichroism (CD) (which is the difference between absorbance of LCP and RCP light and determines χ) spectra are related through the KK relations [22]. Therefore, the complete knowledge of one spectrum allows the calculation of the other. We have noted without verification in Sec. III that the type-I polarization spectra satisfy the KK relations, whereas the type-II spectra do not. Now we will give the numerical evidence and discuss the origin of the difference.

The polarization spectra of Figs. 3 and 4 are revisited in Fig. 9. The dashed curves give the ellipticity χ obtained by numerical simulation, while the dotted curves represent the ellipticity χ' calculated from the θ spectra by KK transformation. Obviously, the χ and χ' curves in Fig. 9(a) are almost the same (the discrepancies at some sharp corners are due to an insufficient number of data points), indicating that the type-I spectra satisfy the KK relations well. However, the χ and χ' curves in Fig. 9(b) are substantially different, showing that the KK relations are not satisfied in the type-II region.

In metallic PCMs, the connection of θ and χ through the KK relations is easy to understand because metals are absorptive, which causes the CD. However, what is the absorption in dielectric PCMs? It is true that there is no absorption in lossless media. Nevertheless, from a grating point of view, the energy in the zero-order diffracted field can be coupled to higher orders if these orders are excited. Since with the term CD one actually concerns the amplitude difference of the LCP and RCP waves, the energy extraction by higher orders can be regarded as a special type of "absorption" of the zero-order energy. Hence CD can still happen and the KK relations hold for the type-I spectra. In the type-II region, however, only the zero-order diffracted waves exist. The zero-order energy cannot be transferred to higher orders and, consequently, the amplitudes of the LCP and RCP waves are always the same. So the ellipticity is definitely zero and the KK relations are not satisfied any more.

V. CONCLUSIONS

A thorough theoretical study of the artificial optical activity in PCM structures was carried out. The general features of polarization conversion in both dielectric and metallic PCMs were analyzed from an effective-medium perspective, by analogy with natural optical activity, and then verified by rigorous numerical simulation based on the electromagnetic theory of gratings.

Numerical results showed that remarkable polarization conversion effects, including giant polarization rotation (tens of degrees) and elliptization, may be realized in the gammadion-shaped nanoparticle arrays with a thickness of

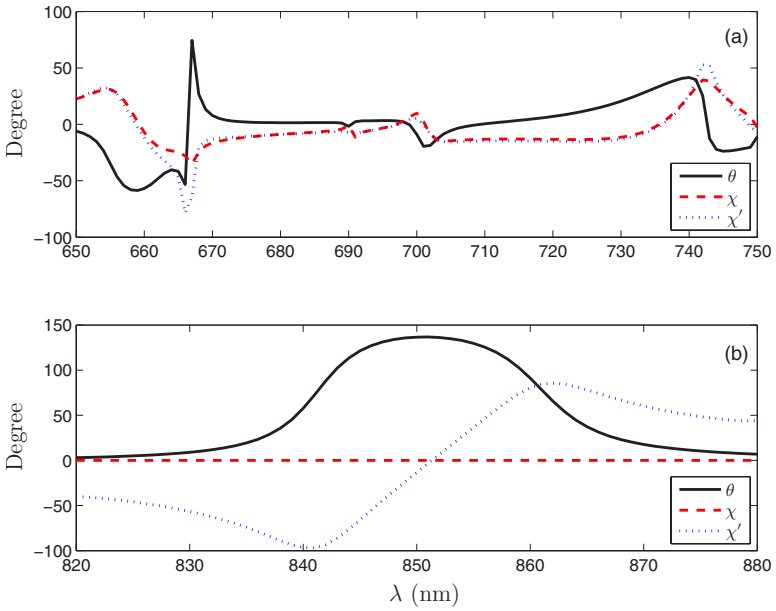

FIG. 9. (Color online) Satisfaction of the type-I (a) and type-II (b) polarization spectra to the KK relations. The solid and dashed curves are the simulated spectra of the polarization rotation angle θ and ellipticity χ; the dotted curves show the ellipticity χ' calculated by KK transformation from the θ curve.

only hundreds of nanometers. The artificial optical activity originates from the circular birefringence in the PCMs, resembling the natural optical activity, and is effectively enhanced by the resonance processes that take place in the PCM structures, i.e., the guided-mode resonance in the dielectric structures and the surface-plasmon resonance in the metallic structures.

The numerical simulation also reveals that the polarization spectra of the dielectric PCMs are clearly divided into two regions separated by the wavelength λ_0 beyond which only the zeroth transmitted order exists: in region I ($\lambda < \lambda_0$), both polarization rotation and elliptization take place and the two spectra satisfy the KK relations; whereas, in region II ($\lambda > \lambda_0$), the ellipticity is always zero and the spectra do not satisfy the KK relations any more. However, the metallic PCMs manifest only the type-I rotation no matter how long the illumination wavelength is. Due to this point and the fact that the transmittance at polarization peaks in metallic PCMs is generally very low, the dielectric PCMs exhibit more potential in applications to be developed as new-generation polarization elements with compact size and diversified functions, such as pure (linear) polarization rotator, half-wave plate, quarter-wave plate, and eighth-wave plate, provided that these numerically predicted polarization properties can be achieved experimentally.

Furthermore, by the analysis of gammadion-shaped nanoparticle arrays at normal incidence, many intriguing features of the polarization properties of PCMs were found: the polarization rotation effect is reciprocal and vanishes in the structures with symmetrical configuration in the normal direction; the effect occurs only in the transmitted field, but not in the reflected field; and, the polarization spectra of two enantiomeric PCM structures are mirror symmetric to each other. Some of these features require the precondition of strict normal incidence. The behavior of PCMs at oblique incidence is much more complicated and needs to be further investigated.

All the general polarization features of PCMs predicted in this paper have been well corroborated by our previous experimental results of metallic PCMs. However, the theoretical predictions for dielectric PCMs, especially the existence of two polarization types and the large rotation angle, still need further experimental verification.

Since the polarization response of PCMs depends heavily on the factors such as structural dimensions, material properties and illumination conditions, an in-depth investigation of their correlation is quite necessary, especially for the purpose of structural design. Our work on the optimization of PCM structures as well as the design of some useful polarization devices for practical applications will be reported elsewhere.

ACKNOWLEDGMENTS

The work was supported by the Academy of Finland (Contracts Nos. 111706, 209806, 106410, and 115781) and the Network of Excellence in Micro-optics (NEMO, www.micro-optics.org).

[1] A. Papakostas, A. Potts, D. M. Bagnall, S. L. Prosvirnin, H. J. Coles, and N. I. Zheludev, Phys. Rev. Lett. **90**, 107404 (2003).

[2] T. Vallius, K. Jefimovs, J. Turunen, P. Vahimaa, and Y. Svirko, Appl. Phys. Lett. **83**, 234 (2003).

[3] M. Kuwata-Gonokami, N. Saito, Y. Ino, M. Kauranen, K. Jefimovs, T. Vallius, J. Turunen, and Y. Svirko, Phys. Rev. Lett. **95**, 227401 (2005).

[4] K. Jefimovs, N. Saito, Y. Ino, T. Vallius, P. Vahimaa, J. Turunen, R. Shimano, M. Kauranen, Y. Svirko, and M. Kuwata-Gonokami, Microelectron. Eng. **78-79**, 448 (2005).

[5] W. Zhang, A. Potts, A. Papakostas, and D. M. Bagnall, Appl. Phys. Lett. **86**, 231905 (2005).
[6] W. Zhang, A. Potts, and D. M. Bagnall, J. Opt. A, Pure Appl. Opt. **8**, 878 (2006).
[7] A. Potts, D. M. Bagnall, and N. I. Zheludev, J. Opt. A, Pure Appl. Opt. **6**, 193 (2004).
[8] M. Born, Proc. R. Soc. London, Ser. A **150**, 84 (1935).
[9] E. U. Condon, Rev. Mod. Phys. **9**, 432 (1937).
[10] A. Yariv and P. Yeh, *Optical Waves in Crystals* (Wiley, New York, 1983), Chap. 4.
[11] *International Tables for Crystallography*, edited by T. Hahn, (Reidel, Dordrecht, The Netherlands, 1983), Vol. A, pp. 92–109.
[12] P. Vincent and M. Nevière, Opt. Acta **26**, 889 (1979).
[13] B. Bai and L. Li, J. Opt. A, Pure Appl. Opt. **7**, 783 (2005).
[14] B. Bai and L. Li, J. Opt. Soc. Am. A **21**, 1886 (2004).
[15] L. Li, J. Opt. Soc. Am. A **14**, 2758 (1997).
[16] L. D. Landau, E. M. Lifshitz, and L. P. Pitaevskii, *Electrodynamics of Continuous Media*, 2nd ed. (Pregamon, Oxford, 1984).
[17] L. Rayleigh, Philos. Mag. **14**, 60 (1907).
[18] S. Peng and G. M. Morris, J. Opt. Soc. Am. A **13**, 993 (1996).
[19] S. M. Norton, T. Erdogan, and G. M. Morris, J. Opt. Soc. Am. A **14**, 629 (1997).
[20] *CRC Handbook of Chemistry and Physics*, edited by R. C. Weast, 64th ed. (CRC Press, Boca Raton, 1984).
[21] L. Li, J. Opt. Soc. Am. A **17**, 881 (2000).
[22] H. Eyring, H. Liu, and D. Caldwell, Chem. Rev. (Washington, D.C.) **68**, 525 (1968).